Materials Letters: X 19 (2023) 100216

Contents lists available at ScienceDirect

Materials Letters: X

journal homepage: www.sciencedirect.com/journal/materials-letters-x

Europium(III) diphenylphosphinate as a potential low-dimensional nanostructured coordination polymer scintillator

Luís Felipe Bricks Bim [1,*], Marco Aurélio Cebim [2]

UNESP, São Paulo State University, Institute of Chemistry, Araraquara, SP 14800-060, Brazil

ARTICLE INFO

Keywords:
XEOL
Scintillation
Nanoscintillator
Rare earth

ABSTRACT

Rare earth diphenylphosphinates – $[RE(dpp)_3]_n$ – are low-dimensional nanostructured luminescent materials with considerable thermal and chemical stability, obtained in powder form, consisting of highly insoluble nanowire/nanorod-shaped particles. As a potential candidate for applications as nanocrystalline scintillator devices, $[Eu(dpp)_3]_n$ has been synthesized by wet route precipitation methodologies. X-ray excited optical luminescence (XEOL) measurements revealed that the samples show intense emission under X-ray excitation, presenting structural and electronic stability against continuous and prolonged exposure to ionizing radiation without changing the chemical environment in which the trivalent europium ion is inserted. Indeed, the self-structuring of $[RE(dpp)_3]_n$ in a polymeric matrix of high thermal stability allowed $[Eu(dpp)_3]_n$ to be a low-dimensional nanostructured luminescent coordination polymer resistant to *radiation damage*.

1. Introduction

Scintillators are a unique class of down-conversion optical materials capable of absorbing high-energy (ionizing) radiation and efficiently converting it into ultraviolet, visible, or near-infrared radiation [1,2]. In this context, one can cite a class of emerging nanomaterials known as nanocrystalline scintillators (NCSs), including but not limited to quantum dots, nanoclusters, metal–organic frameworks, and nanophosphors. NCSs differ from others in dimensionality, which translates into significant differences in defect density and the availability of the effective energy states to electrons [3]. Over the past few decades, many studies have addressed the usage of scintillators for classical applications such as ionizing radiation detection and non-destructive security inspection [4]. However, current interest is centered on developing nanoscintillators that serve a dual purpose: as scintillators themselves and as photosensitizers (cytotoxic reactive oxygen species – ROS – generators, most importantly singlet oxygen, $^1O_2$) for X-ray-induced photodynamic therapy (X-PDT) applications [2,3,5,6].

As potential candidates for the applications above, rare earth diphenylphosphinates – $[RE(dpp)_3]_n$ – are low-dimensional nanostructured coordination polymers that present considerable thermal and chemical stability, resembling the behavior of inorganic phosphates [7]. By combining those intriguing characteristics with the high energy conversion efficiency and energy resolution of metal ion-based emitters [8], as well as the plentiful ladder-like energy levels from RE ions [2], one can help to obtain 1D-nanostructured rare earth-based scintillators with control of shape and particle size as a function of the synthesis methodology. Thus, it is expected to improve the scintillation efficiency due to the RE activator's high atomic number and fast decay owing to the polymeric matrix organized in a nanostructure of one-dimensional nanorods (NR; $R_{length(\ell)/diameter(d)} < 10$) or nanowires (NW; $R_{\ell/d} > 10$).

2. Material and methods

$[Eu(dpp)_3]_n$ has been synthesized by wet route precipitation methodologies, according to [7]. The wet route synthesis (WRS) consists of a direct reaction between a rare earth chloride ($RECl_3$) and diphenylphosphinic acid (H*dpp*) in a 1:1 ethanol-to-water mixture @ 1:3 metal-to-ligand ratio under dynamic $N_{2(g)}$ atmosphere; the $RECl_3$ solution is slowly dripped onto the ligand solution under constant stirring, causing the $[RE(dpp)_3]_n$ to precipitate. Modifications through U-WRS (ultrasound-assisted wet route synthesis), M-WRS (modulator-assisted wet route synthesis), and S-WRS (wet route synthesis with solvothermal treatment) lead to changes in precipitation kinetics, crystalline phase

* Corresponding author.
E-mail addresses: luis.bim@unesp.br, felipebricks@gmail.com (L.F.B. Bim), marco.cebim@unesp.br (M.A. Cebim).
[1] https://orcid.org/0000-0003-2160-7795.
[2] https://orcid.org/0000-0001-8267-935X.

https://doi.org/10.1016/j.mlblux.2023.100216
Received 30 December 2022; Received in revised form 27 March 2023; Accepted 19 August 2023
Available online 28 August 2023

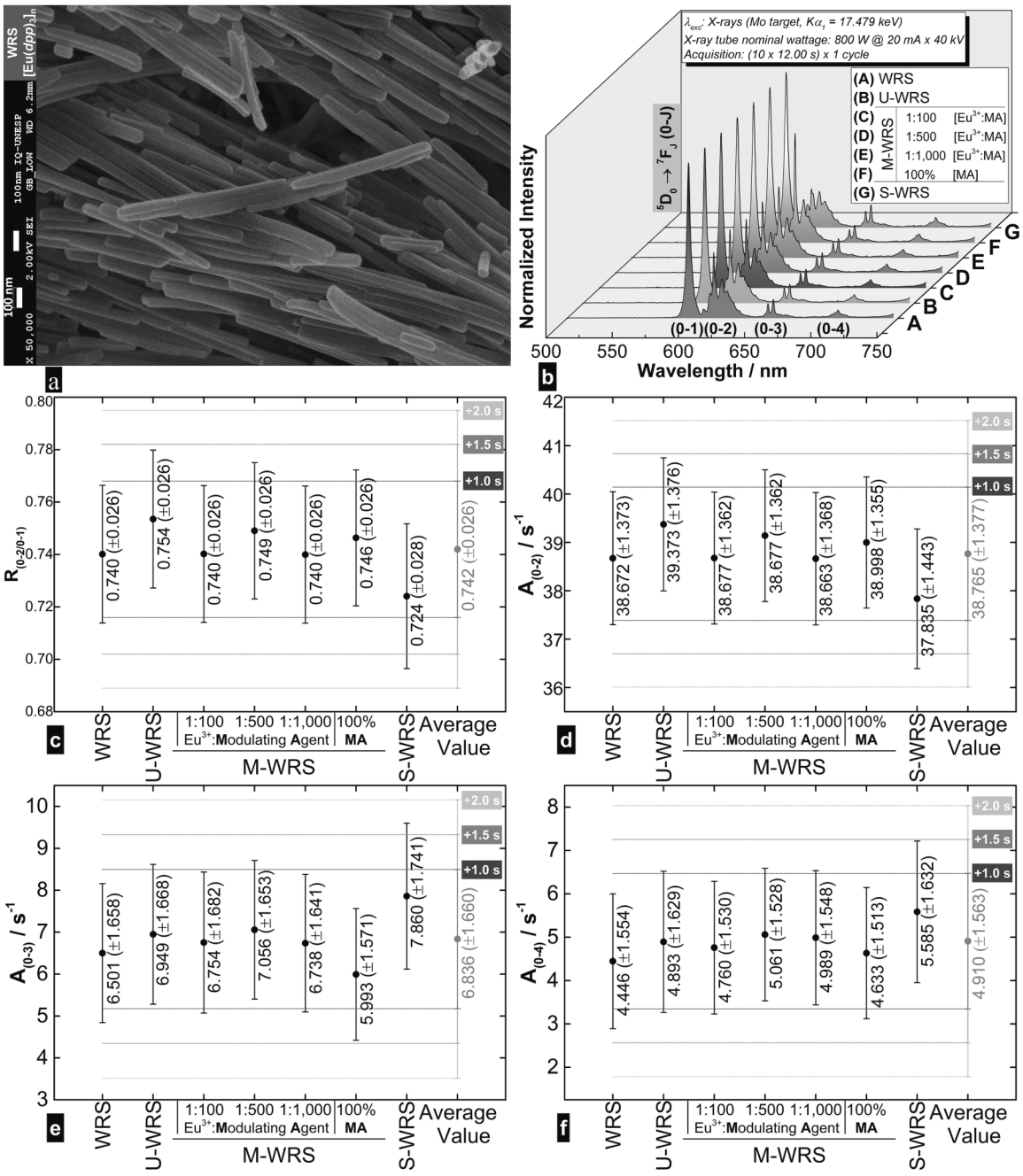

Fig. 1. (a) SEM-FEG photomicrography of WRS $[Eu(dpp)_3]_n$, **(b)** XEOL spectra, **(c)** integrated intensity ratio $R_{(0-2/0-1)} = I(^5D_0 \rightarrow ^7F_2)/I(^5D_0 \rightarrow ^7F_1)$, and **(d-f)** individual radiative decay rate $A_{(0-J)}$: $A_{rad}^{^5D_0 \rightarrow ^7F_2}, A_{rad}^{^5D_0 \rightarrow ^7F_3}, A_{rad}^{^5D_0 \rightarrow ^7F_4}$, for WRS/U-WRS/M-WRS/S-WRS $[Eu(dpp)_3]_n$ @ room temperature.

formation rate or facilitating interaction between reaction components. It is noteworthy that the M-WRS methodology was carried out in the presence of different amounts of methanoic acid as a coordination modulating agent (MA): 1:100, 1:500, and 1:1,000 Eu^{3+}:MA; another situation was also explored in which the ethanol/water solvent was utterly replaced by methanoic acid (100% MA). *Purity and brands*: $EuCl_3$ solution was obtained by stoichiometric hydrochloric acid (Sigma-Aldrich, 37%) attack on Eu_2O_3 (Aldrich, 99.99%), and its concentration was determined by complexation titrimetry; *ligand*: diphenylphosphinic acid (Aldrich, ≥98.0%); *modulating agent (MA)*: methanoic acid (Sigma-Aldrich, ≥95%); *solvent:* ethanol (Sigma-Aldrich, ≥99.5%) and Milli-Q® ultrapure water (18.2 MΩ·cm @ 25 °C); *atmosphere*: compressed nitrogen gas (White Martins, 99.998%).

2.1. X-ray excited optical luminescence (XEOL) measurements

The samples were exposed to the X-ray beam (*bremsstrahlung continuum* and characteristic X-rays) generated by a Rigaku X-ray diffractometer, with a static Molybdenum anode as target and operated at a tube wattage rating of 800 W @ 20 mA × 40 kV (nominal electrical quantities); true electrical quantities (DCA, DCV, wattage) were continuously monitored over operating time. Sample luminescence was collected in *front-face* mode through a one-way multicore fiber-optic bundle. Further details on the construction of the XEOL system can be found in [9].

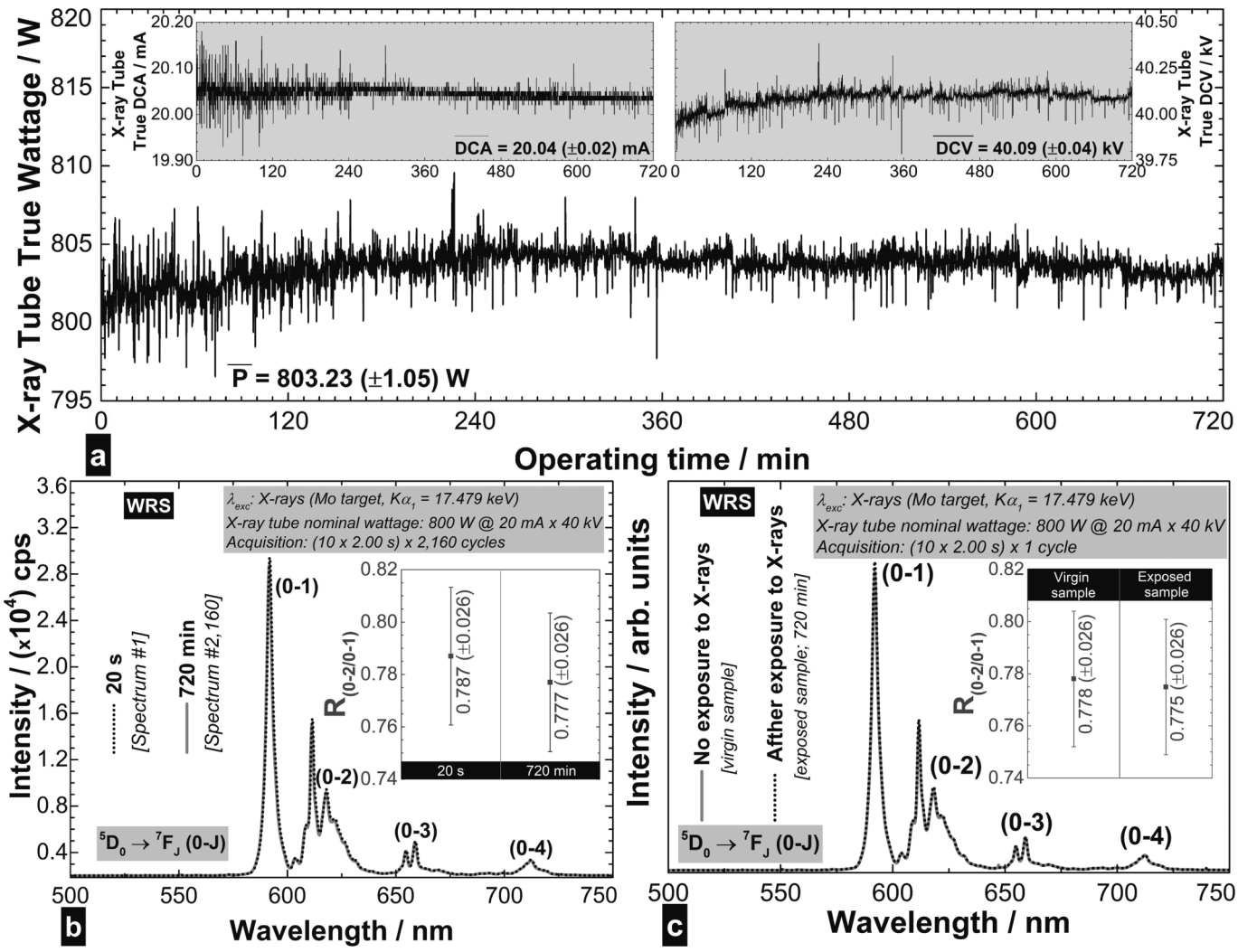

Fig. 2. **(a)** X-ray tube true electrical quantities over operating time, **(b)** XEOL damage spectra for WRS $[Eu(dpp)_3]_n$ @ room temperature after 20 s and 720 min of continuous exposure, and **(c)** XEOL emission spectra for a virgin and an exposed (720 min) WRS $[Eu(dpp)_3]_n$ sample.

2.2. Calculation

The radiative rates of spontaneous emission A_{0J} were determined from the $^5D_0 \rightarrow {}^7F_2$, $^5D_0 \rightarrow {}^7F_3$, and $^5D_0 \rightarrow {}^7F_4$ transitions, respectively. The $^5D_0 \rightarrow {}^7F_1$ transition was taken as the reference and the A_{01} value is estimated to be $50 s^{-1}$. In this way, A_{0J} rates were calculated from the intensity ratios (I_{0J}) between $^5D_0 \rightarrow {}^7F_J (J = 2, 3, 4)$ and $^5D_0 \rightarrow {}^7F_1 (I_{01})$ transitions using the expression $A_{0J} = A_{01}\left(\frac{I_{0J}}{I_{01}}\right)\left(\frac{\nu_{01}}{\nu_{0J}}\right)$, where ν_{0J} is the energy barycenter of the transition [10].

3. Results and discussion

$[RE(dpp)_3]_n$ are low-dimensional nanostructured rare earth-based materials with potential application as NCSs devices. Such nanomaterials have considerable thermal and chemical stability, comparable to inorganic phosphates, obtained – as a function of WRS methodologies – with well-defined morphology, size, and optical properties.

Specifically, $[Eu(dpp)_3]_n$ is a 1D1-nanostructured luminescent coordination polymer obtained in powder form as a finely-divided white solid consisting of highly insoluble nanowire-shaped particles. The morphological behavior of WRS $[Eu(dpp)_3]_n$ (Fig. 1**(a)**) should be regarded as representative of the entire Eu^{3+} series synthesized through WRS methodologies. The particles' shape is kept unaltered, differing only in terms of dimensions (length & diameter) which always present $R_{\ell/d} > 10$. Therefore, they can be classified as nanowires regardless of the adopted WRS methodology.

The XEOL spectra for $[Eu(dpp)_3]_n$ synthesized by WRS methodologies are shown in Fig. 1**(b)**. The general behavior of the samples is quite similar, regardless of the synthesis methodology; indeed, solids show the same spectral profile under X-ray excitation (Mo target, $K_{\alpha_1} = 17.479$ keV; 800 W @ 20 mA × 40 kV, nominal values), following the same trend of photoluminescence spectroscopy (UV–Vis PLS) [7]. It is possible to verify relaxations of the first Eu^{3+} excited state (*emitting level*), $^5D_0$, to four ^7F_J levels, $^5D_0 \rightarrow {}^7F_{J=1,2,3,4}$; for simplicity, these transitions are assigned as (0-J) in the spectra. The $^5D_0 \rightarrow {}^7F_0$ transition is not observed, and transitions $^5D_0 \rightarrow {}^7F_5$ and $^5D_0 \rightarrow {}^7F_6$ are outside the monitored spectral range.

Previous UV–Vis PLS studies have already pointed to the existence of at least two symmetry sites in $[RE(dpp)_3]_n$ structure, both in Eu^{3+}-doped matrices [11] and in a pure $[Eu(dpp)_3]_n$ matrix synthesized by WRS methodologies [7]. Nevertheless, the XEOL emission process for $[Eu(dpp)_3]_n$ is always governed by Eu^{3+} ions from higher symmetry sites, resulting in the integrated intensity ratios $R_{(0-2/0-1)} = I(^5D_0 \rightarrow {}^7F_2)/I(^5D_0 \rightarrow {}^7F_1) = 0.742$ (±0.026) as an average value (AV) (Fig. 1**(c)**); individual $R_{(0\text{-}2/0\text{-}1)}$ results for each sample are similar to each other, with standard deviations no greater than ± 2.0 s of AV. The contribution of the less symmetrical sites to the Eu^{3+} ion emission under X-ray

excitation never becomes preponderant in any WRS methodologies.

Individual radiative decay rates from the $^5D_0$ excited state to the low-lying $^7F_{J=2,3,4}$ states under X-ray excitation are presented in Fig. 1**(d-f)**; the $^5D_0 \rightarrow {}^7F_1$ transition is governed by magnetic dipole mechanisms, which makes it independent of the ligand field (*site-independent*) and results in constant emission intensity. Overall, the most significant contribution to $A_{rad}^{(total)}$ comes from $A_{rad}^{^5D_0 \rightarrow {}^7F_2}$ with an AV of 38.765 ($\pm$1.377) s^{-1}.

Radiation damage measurements were performed for WRS [Eu(*dpp*)$_3$]$_n$ as a structural and electronic stability test to verify the effects of continuous and prolonged exposure of the solid to the X-ray beam. X-ray tube true electrical quantities were continuously monitored over the 720-min operating time, effectively corresponding to 803.23 ($\pm$1.05) W @ 20.04 ($\pm$0.02) mA $\times$ 40.09 ($\pm$0.04) kV (Fig. 2**(a)**); such parameter values, with standard deviations smaller than 0.15%, attest to the stability of the XEOL system.

XEOL *damage* spectra for WRS [Eu(dpp)$_3$]$_n$ @ room temperature show intense emission (>2.8 10^4 cps) under X-ray excitation (Fig. 2**(b)**), an essential property for its application as NCS. After 720 min of continuous exposure to the X-ray beam, there was no appreciable change in the chemical environment (*local symmetry*) in which the Eu^{3+} ion is inserted since the $R_{(0\text{-}2/0\text{-}1)}$ ratio remained practically constant @ 20 s [*spectrum #1*] and 720 min [*spectrum #2,160*], with a slight decrease of 1.3% in absolute values. The spectral profile and the emission intensity remained conserved over exposure time, suggesting that [Eu(*dpp*)$_3$]$_n$ is a *radiation damage* tolerant nanomaterial. As proof of concept, the same stability behavior is observed when comparing a virgin (no exposure to X-rays) and an exposed (720 min) WRS [Eu(*dpp*)$_3$]$_n$ sample, resulting in $R_{(0\text{-}2/0\text{-}1)}$ = 0.778 ($\pm$0.026) and 0.775 ($\pm$0.026), respectively (Fig. 2**(c)**).

4. Conclusion

[Eu(*dpp*)$_3$]$_n$ samples show intense emission under X-ray excitation, with considerable stability verified against prolonged exposure to ionizing radiation. After 720 min of continuous exposure to the X-ray beam, there was no appreciable change in the chemical environment (*local symmetry*) in which Eu^{3+} is inserted, verified by conserving the XEOL spectral emission profile. The spectral profile and the emission intensity remained conserved over exposure time, suggesting that [RE(*dpp*)$_3$]$_n$ are nanomaterials resistant to *radiation damage*. Critical to a potential application as NCSs devices, the self-structuring of [RE(*dpp*)$_3$]$_n$ in a polymeric matrix of high thermal stability, formed by nanostructures of one-dimensional nanorods or nanowires, allowed such low-dimensional nanostructured luminescent coordination polymers to present structural and electronic stability against continuous and prolonged exposure to X-rays.

CRediT authorship contribution statement

Luís Felipe Bricks Bim: Conceptualization, Methodology, Investigation, Writing – original draft, Writing – review & editing. **Marco Aurélio Cebim:** Software, Writing – review & editing, Supervision.

Declaration of Competing Interest

The authors declare that they have no known competing financial interests or personal relationships that could have appeared to influence the work reported in this paper.

Data availability

Data will be made available on request.

Acknowledgments

This study was financed in part by the *Coordenação de Aperfeiçoamento de Pessoal de Nível Superior – Brasil* (CAPES) – Finance Code 001.

References

[1] J.-C.-G. Bünzli, Lanthanide-doped nanoscintillators, Light Sci. Appl. 11 (2022) 285, https://doi.org/10.1038/s41377-022-00987-2.
[2] L. Lei, Y. Wang, A. Kuzmin, Y. Hua, J. Zhao, S. Xu, P.N. Prasad, Next generation lanthanide doped nanoscintillators and photon converters, ELight 2 (2022), https://doi.org/10.1186/s43593-022-00024-0.
[3] S.K. Gupta, Y. Mao, Recent advances, challenges, and opportunities of inorganic nanoscintillators, Front. Optoelectron. 13 (2020) 156–187, https://doi.org/10.1007/s12200-020-1003-5.
[4] M. Nikl, A. Yoshikawa, Recent R&D trends in inorganic single-crystal scintillator materials for radiation detection, Adv. Opt. Mater. 3 (2015) 463–481, https://doi.org/10.1002/adom.201400571.
[5] W. Sun, Z. Zhou, G. Pratx, X. Chen, H. Chen, Nanoscintillator-mediated X-ray induced photodynamic therapy for deep-seated tumors: from concept to biomedical applications, Theranostics 10 (2020) 1296–1318, https://doi.org/10.7150/thno.41578.
[6] X. Wang, W. Sun, H. Shi, H. Ma, G. Niu, Y. Li, J. Zhi, X. Yao, Z. Song, L. Chen, S. Li, G. Yang, Z. Zhou, Y. He, S. Qu, M. Wu, Z. Zhao, C. Yin, C. Lin, J. Gao, Q. Li, X. Zhen, L. Li, X. Chen, X. Liu, Z. An, H. Chen, W. Huang, Organic phosphorescent nanoscintillator for low-dose X-ray-induced photodynamic therapy, Nat. Commun. 13 (2022) 5091, https://doi.org/10.1038/s41467-022-32054-0.
[7] L.F.B. Bim, E.B. Stucchi, M.A. Cebim, A new overview on rare earth diphenylphosphinates: Europium characteristic luminescence of low dimensional nanostructured materials, J. Lumin. 203 (2018) 105–112, https://doi.org/10.1016/j.jlumin.2018.06.040.
[8] Y. Wang, X. Yin, J. Chen, Y. Wang, Z. Chai, S. Wang, Gleaming uranium: an emerging emitter for building X-ray scintillators, Chem. Eur. J. 26 (9) (2020) 1900–1905.
[9] M.A. Cebim, H.H. De Souza Oliveira, N. Barelli, M.R. Davolos, System for X-Ray excited optical luminescence (XEOL) measurements, Quim. Nova 34 (2011) 1057–1062, https://doi.org/10.1590/S0100-40422011000600024.
[10] G.F. de Sá, O.L. Malta, C. de Mello Donegá, A.M. Simas, R.L. Longo, P.A. Santa-Cruz, E.F. da Silva, Spectroscopic properties and design of highly luminescent lanthanide coordination complexes, Coord. Chem. Rev. 196 (1) (2000) 165–195.
[11] E.M. Abreu, C.S. Francisco, S.I. Klein, E.B. Stucchi, Strongly luminescent, highly ionic europium in a lanthanum diphenylphosphinate matrix, Opt. Mater. (Amst) 35 (2013) 332–337, https://doi.org/10.1016/j.optmat.2012.08.003.